

**EXPERIMENTAL STUDY ON DUCTILE PRECAST END-DIAPHRAGMS OF  
SLAB-ON-GIRDER CONCRETE BRIDGES: PRE-TEST ANALYTICAL STUDY.**

**Esteban Villalobos Vega, C.E.**, Bridge Program, PITRA-LanammeUCR, Costa Rica

**Guillermo Santana Barboza, PhD**, Executive President, INCOFER, Costa Rica

**Roy Barrantes Jiménez, C.E.**, Bridge Program Coordinator, PITRA-LanammeUCR, Costa  
Rica

**ABSTRACT**

Even if the failure of diaphragms on concrete bridges has not been widely reported on past earthquakes, 2010 Chile earthquake demonstrated the importance of its use and the need of developing and understanding a viable and clear seismic load path. Nevertheless, both experimental work and seismic design provisions for diaphragms on concrete bridges are very limited. The present study proposes the use of ductile precast concrete end-diaphragms made with the hybrid system, i.e., unbonded post-tension in combination with mild steel reinforcement that acts as a fuse in the transverse direction by having a yield resistance less than the substructure resistance. The project includes the proposal of a simplified seismic analysis of slab-on-girder concrete bridges with ductile precast end-diaphragms, in order to design and predict the behavior of the entire structural system. The final step will be the laboratory cyclic test of a full-size specimen corresponding to 0,6m length of a case study bridge end that will include the interaction between all the components. This solution could be implemented in new bridges as a part of completely Accelerated Bridge Construction (ABC) proposals, or in the case where it is necessary to seismically retrofit concrete bridges when they get old or damaged.

**Keywords:** Accelerated Construction, Connections, Creative/Innovative Solutions and Structures, Designing and Testing Related to Seismic, Research.

## INTRODUCTION

Out of the total number of bridges that make up the Costa Rican national inventory, 78% are bridges constructed in concrete at least on its superstructure, and more than 75% are simple supported bridges with a length under 35m. Most of these structures were designed and constructed prior to the 80's, which implies that they were conceived when the level of knowledge and awareness of seismic performance was inadequate compared with current understanding. Consequently, many of these bridges are of high importance when speaking about high seismic vulnerability.

It is also noticeable that these structures are old and due to the lack of maintenance, they are in an evident state of deterioration. Even if it is obvious that something must be done, it seems unlikely that all these bridges will be replaced, even in a long term program. Instead, it would be more feasible to think about retrofitting of a portion of the bridges to increase their service lives, taking into consideration the previously mentioned seismic vulnerability.

Another paradigm that has gained strength in recent years is the public concern about road closures, as a result of construction, substitution or retrofit of bridges. The consequences of these works could be economic losses, security concerns at the construction site, costs and delay time suffered by the users, and in general problems that worsen the public perception of the transportation agency. At the same time, due to current environmental awareness, there is a concern about unnecessary use of vehicles operating on fossil fuels. In this context, the use of Accelerated Bridge Construction (ABC) presents a unique opportunity to overcome these issues in an efficient and durable manner, which over the years and with the gain in experience in its use, will be more and more competitive compared to traditional solutions. However, in a country like Costa Rica located in a high seismic area with frequent earthquakes, great care must be taken in the way the connections between precast elements are made: connections probably will require experimental testing. This practice is frequently called SABC (Seismic Accelerated Bridge Construction).

In the case of steel bridges, during the last two decades some important distress suffered by the superstructure and mainly by the substructure during the most important earthquakes that occurred worldwide has been identified<sup>1</sup>. As a proposal to solve these problems through retrofit, Zahrai and Bruneau<sup>1</sup> developed a system of ductile end-diaphragms for slab-on-girders steel bridges. They tested three types of diaphragms based on three successful bracing frames systems for buildings<sup>2</sup>. Furthermore, they proposed a simplified design procedure based on analytical evidence on 2-D and 3-D computational models. The solution has evolved until it became the Type 2 Global Seismic Design Strategy (GSDS) of the AASHTO Guide Specifications for LRFD Seismic Bridge Design<sup>3</sup> that applies only to steel superstructures, and likewise it forms part of other important seismic design and retrofit codes in USA.

Even if the failure of diaphragms on concrete bridges has not been widely reported on past earthquakes, the 2010 Chile earthquake came to demonstrate the importance of its use and the need of developing and understanding a viable and clear seismic load path in bridges<sup>4</sup>.

Nevertheless, according to the author knowledge and research, both experimental work and seismic design provisions for diaphragms on concrete bridges are very limited. Therefore, following the concept proposed by Zahrai and Bruneau<sup>1</sup> for steel bridges, it would be important not only to develop guidelines in the behavior and detailing of concrete diaphragms for seismic resistance, but to explore the use of concrete ductile diaphragms as fuses (Type 2 GSDS) in the seismic resistance of concrete bridges as part of ABC solutions for retrofitting of old infrastructures, design of new bridges or even a combination of both in the case of simple supported concrete bridges.

## PROPOSED SOLUTION

Although specifications regarding the design and detailing of standard concrete diaphragms are basic and rare, Fig. 1(a) shows the typical schematic that is used, where the longitudinal reinforcing steel pass through precast beams, transverse reinforcing steel is developed in the CIP slab, and depth varies from middle to almost the entire precast beam height. The main idea behind this schematic seems to meet the seismic load transfer from superstructure to substructure without any damage at the diaphragm-beam-slab system. The later could be one of the reasons why it is difficult to find reports on concrete diaphragm damages during past earthquakes. However, another consequence of this approach is that generally the strength or threshold of unacceptable damage of the substructure considering both supports, as the piers, such as abutments, is less than the strength of the diaphragm-beam-slab system, causing damage in the substructures as it has been observed in important earthquakes worldwide.

Similar to what Zahrai and Bruneau<sup>1</sup> did in their work for steel bridges, it is possible to use a proven successful solution for seismic resistance of concrete precast buildings in order to propose ductile precast end-diaphragms that acts as a fuse in the transverse direction by having a yield resistance less than the substructure resistance. The solution implies a global rocking mechanism through the use of two connections (see Fig. 1(b)): (a) For the diaphragm-to-beam connection an hybrid joint will be used in order to have adequate energy dissipation, re-centering capability, and low damaged; (b) For the beam-to-slab connections a partially restrained (PR) moment joint will be used in order to allow the joint to rotate with the minimum moment resistance possible and the damage will be in the form of yielding of the steel angles, condition that can be designed and controlled .

Notice that in this case, the concrete slab should be precast in order to generate the opening of the joint in a controlled manner, regardless of whether the project is a retrofit or a new project.

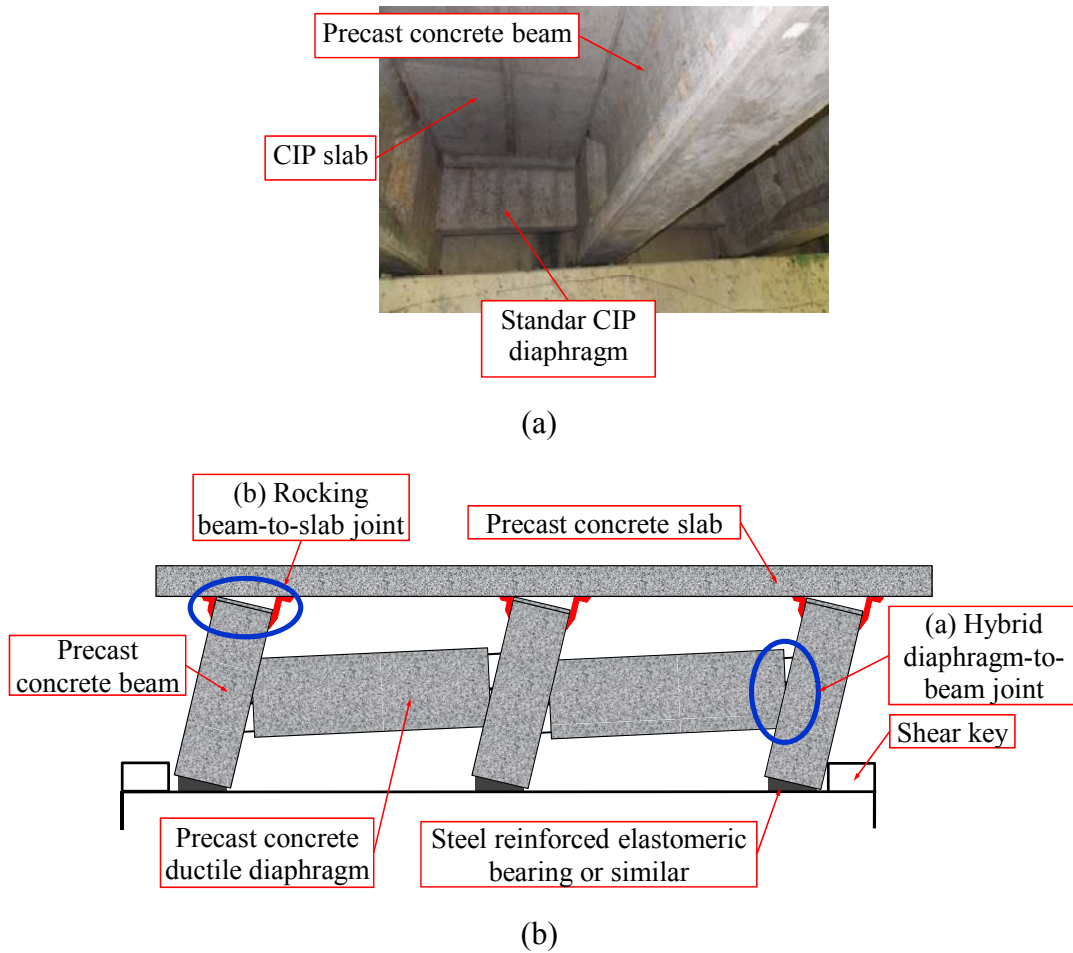


Fig. 1 Concrete diaphragm`s approaches: (a) Standard concrete diaphragm practice; (b) Rocking system proposal.

It must be clear that the solution presented is regarding the transverse end section showed in Fig. 1(b). The actual seismic behavior in the transverse direction of the bridge in 3-D is not taken into account in this project. There is a distance measured from the end of the beam where it goes from the rotated position showed in Fig. 1(b) until a displaced but almost zero rotation stage. The consequences of this behavior are of major importance on the behavior and performance of the bridge and should be of concern future research either analytical or experimental.

## ANALYTICAL APPROACH

## (a) HYBRID DIAPHRAGM-TO-BEAM JOINT

As a result of a series of extensive analytical and experimental research projects during the late 80's and early 90's, beginning with the NIST initiative and finishing with the PRESS program<sup>5</sup>, the hybrid system emerged as a practical, competitive and high performance solution to the concern of behavior of precast concrete connections during earthquakes.

As is shown in Fig.2, the system centers its behavior almost exclusively in the opening of the joint in between the elements of the connection, bridge beam and diaphragm. In order to achieve its purpose, the system is composed of: (i) Post-tensioning steel at the middle of the diaphragm's cross section that is unbonded from anchorage to anchorage, which provides re-centering capability to the joint; (ii) The same amount of mild steel reinforcement in the top and bottom of the cross section with a debonded length in the joint to avoid premature low-cyclic fatigue failure of the rebars, which provide energy dissipating capability to the joint. Additionally it is used a grout pad in the interface between elements to take into account constructive tolerances, and to keep the integrity of the joint due to the development of high compression stresses.

In order to describe the behavior of the hybrid joint, consider Fig. 2(a). The total rotation or drift of the bridge beams,  $\alpha'$ , is shown as a relative displacement between diaphragms,  $\Delta_T$ , which could be either the yield or ultimate displacement condition. The total displacement is composed of an inelastic component,  $\Delta_i$ , and an elastic component,  $\Delta_e$ . The inelastic component is responsible for the rotation of the joint, and the sum of both, elastic ( $\theta_e$ ) and inelastic ( $\theta$ ) components, make up the total rotation of the diaphragm,  $\theta_v$ . The latter supposes that the concrete of the body of the diaphragm does not suffer considerable cracking during the earthquake up to the failure of the joint, which has been proven in past tests<sup>5</sup>.

Building on the work by Restrepo and Rahman<sup>6</sup> on structural hybrid walls, the yield state is characterized by the total yield displacement,  $\Delta_{vy}$ , total yield shear,  $V_{vy}$ , and initial elastic stiffness,  $K_{iv}$ , and can be computed as follows (SI units):

$$\Delta_{vy} = \frac{V_{vy} \cdot L_v^3}{12 \cdot E_c \cdot I_g} \cdot \left( 1 + \frac{36 \cdot I_g}{A_g \cdot L_v^2} \right) + \frac{\varepsilon_{sh} \cdot L_u}{(1 - \xi) \cdot d_{st}} \cdot L_v \quad (1)$$

$$V_{vy} = \frac{1}{L_v} \cdot [T_{pe} \cdot (h_v - \beta_1 \cdot \xi \cdot d_{st}) + T_{sty} \cdot d_{st} \cdot (2 - \beta_1 \cdot \xi)] \quad (2)$$

$$K_{iv} = \frac{[T_{pe} \cdot (h_v - \beta_1 \cdot \xi \cdot d_{st}) + T_{sty} \cdot d_{st} \cdot (2 - \beta_1 \cdot \xi)]}{\frac{[T_{pe} \cdot (h_v - \beta_1 \cdot \xi \cdot d_{st}) + T_{sty} \cdot d_{st} \cdot (2 - \beta_1 \cdot \xi)] \cdot L_v^3}{12 \cdot E_c \cdot I_g} + \frac{\varepsilon_{sh} \cdot L_u}{(1 - \xi) \cdot d_{st}} \cdot L_v^2} \quad (3)$$

where  $E_c$  is the modulus of elasticity of diaphragm concrete;  $L_v$  is the length of the concrete precast diaphragm;  $I_g$  is the moment of inertia of the gross diaphragm cross section;  $A_g$  is the

gross area of the diaphragm cross section;  $L_u$  is the intentional unbonded length of mild steel;  $\epsilon_{sh}$  is the strain in the mild steel reinforcing at the onset of strain hardening;  $d_{st}$  is the effective depth of the mild steel reinforcing in tension;  $\xi$  is a parameter to approximate the neutral axis;  $h_v$  is the overall diaphragm height;  $T_{pe}$  is the total effective force in the post-tensioning steel after losses;  $T_{sty}$  is the total yield force in the mild-steel reinforcing in tension;  $\beta_1$  is the parameter of the concrete rectangular stress block.

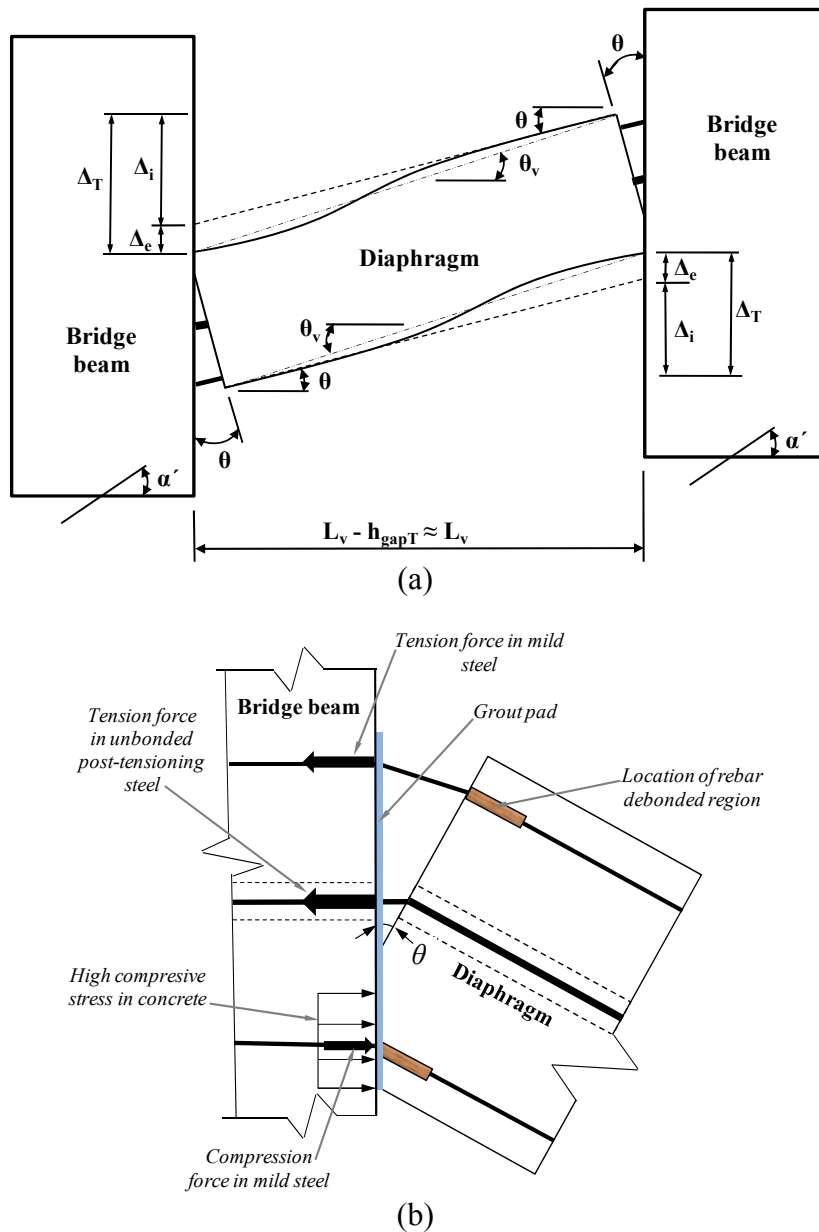


Fig. 2 Ductile precast end-diaphragm system: (a) General idealized deformed shape of one ductile precast end-diaphragm; (b) Idealized deformed shape of the hybrid joint (The term  $h_{gapT}$  is the total width of grout pad in both diaphragm ends).

Similarly, the ultimate state (mild steel tension reinforcement failure due to low cyclic fatigue) is characterized by the total ultimate displacement,  $\Delta_{vu}$ , and total ultimate shear,  $V_{vu}$ , and can be obtained by (SI units):

$$\Delta_{vu} = \frac{V_{vu} \cdot L_v^3}{12 \cdot E_c \cdot I_g} \cdot \left( 1 + \frac{36 \cdot I_g}{A_g \cdot L_v^2} \right) + \frac{\varepsilon_{sh} \cdot (L_u + \alpha_b \cdot d_{bt})}{d_{st} \cdot (1 - \xi) - c_c} \cdot L_v \quad (4)$$

$$V_{vu} = \frac{1}{L_v} \cdot \left[ T_{py} \cdot (h_v - 2 \cdot c_c - \xi \cdot d_{st}) + 2 \cdot T_{stu} \cdot \left( d_{st} - c_c - \frac{\xi \cdot d_{st}}{2} \right) \right] \quad (5)$$

where  $\alpha_b$  is the coefficient quantifying the effective additional debonded length in the mild steel reinforcing;  $d_{bt}$  is the diameter of reinforcing bar;  $c_c$  is the concrete cover to side of transverse reinforcement;  $T_{py}$  is the total yield force in the post-tensioning steel;  $T_{stu}$  is the total ultimate force in the mildsteel reinforcing at failure.

## (b) ROCKING BEAM-TO-SLAB JOINT

Based on the behavior of partially restrained (PR) connections widely use in steel building construction, Fig. 3 shows the concept of the behavior of the joint. As the slab is moved horizontally by the seismic action, the connection opens at the interface haunch-precast slab with a low moment capacity. Once the joint starts to open the tension angle undergoes double curvature bending between the horizontal and vertical leg. There is a point where both sides of the tension angle are plasticized and begin to dissipate energy: a global plastic hinge is formed in the joint.

Another consideration of the rocking beam-to-slab joint is that the interface in between steel angle-precast slab and steel angle-precast beam should be design as slip critical connections for the interface shear transfer in order to have composite action for gravity loads and vehicular live load along the entire bridge length.

For this joint, the proposal is based in the work of Weldon and Kurama<sup>7</sup>, who developed a solution for precast coupling beams using unbonded post-tensioning steel like in the hybrid system, with steel top and seat angles used at the beam ends to yield and provide energy dissipation during the earthquake.

The yield state is characterized by the total yield rotation,  $\alpha_{ay}$ , total yield moment,  $M_{ay}$ , and the initial elastic rotational stiffness,  $K_{iaa}$ , and can be written as (SI units):

$$\alpha_{ay} = \frac{\left( \frac{f_{ay} \cdot l_a \cdot t_a^2 \cdot l_{g1}^3}{6 \cdot l_{g2} \cdot E_{as} \cdot l_a} \right) \cdot \left( 1 + \frac{0.78 \cdot t_a^2}{l_{g1}^2} \right)}{\left( b_b + \frac{t_a}{2} \right)} \quad (6)$$

$$M_{ay} = \frac{1}{2} \cdot \left[ \left( N_{at} \cdot \left( \frac{f_{ay} \cdot l_a \cdot t_a^2}{2 \cdot l_{g2}} \right) + P_{tl} \right) \cdot b_b + \left( \frac{f_{ay} \cdot l_a \cdot t_a^2}{2 \cdot l_{g2}} \right) \cdot N_{at} \cdot (b_b + t_a) \right] \quad (7)$$

$$K_{ia\alpha} = \frac{3 \cdot l_{g2} \cdot E_{as} \cdot I_a \cdot (b_b + \frac{t_a}{2}) \cdot \left[ N_{at} \cdot \left( \frac{f_{ay} \cdot l_a \cdot t_a^2}{2 \cdot l_{g2}} \right) + P_{tl} \right] \cdot b_b + \left( \frac{f_{ay} \cdot l_a \cdot t_a^2}{2 \cdot l_{g2}} \right) \cdot N_{at} \cdot (b_b + t_a)}{f_{ay} \cdot l_a \cdot t_a^2 \cdot l_{g1}^3 \cdot \left( 1 + \frac{0.78 \cdot t_a^2}{l_{g1}^2} \right)} \quad (8)$$

where  $b_b$  is the bridge beam width;  $t_a$  is the angle leg thickness;  $f_{ay}$  is the angle steel yield strength;  $l_a$  is the angle length;  $l_{g1}$  is the length of horizontal angle leg assumed to act as a cantilever;  $l_{g2}$  is the effective gage length;  $E_{as}$  is the Young's modulus for angle steel;  $I_a$  is the moment of inertia for angle leg cross-section;  $N_{at}$  is the number of steel angles in tension;  $P_{tl}$  is the tributary weight of the slab.

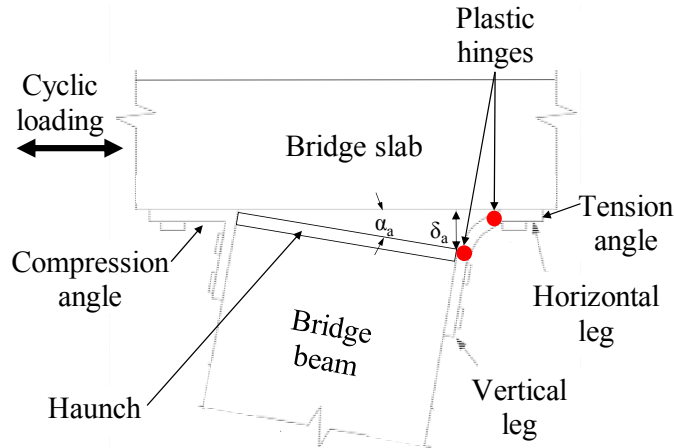


Fig. 3 Idealized deformed shape of the rocking beam-to-slab joint.

Similarly, the maximum probable capacity state is characterized by the total maximum probable rotation,  $\alpha_{as}$ , and the total maximum probable moment,  $M_{as}$ , and is given by the following expressions (SI units):

$$\alpha_{as} = \varphi_{\delta} \cdot \alpha_{ay} \quad (9)$$

$$M_{as} = \frac{1}{2} \cdot \left[ \left( N_{at} \cdot \left( \varphi_T \cdot \left[ \frac{f_{ay} \cdot l_a \cdot t_a^2}{2 \cdot l_{g2}} \right] \right) + P_{tl} \right) \cdot b_b + \varphi_T \cdot \left[ \frac{f_{ay} \cdot l_a \cdot t_a^2}{2 \cdot l_{g2}} \right] \cdot N_{at} \cdot (b_b + t_a) \right] \quad (10)$$

where  $\varphi_{\delta}$  is a constant based on experimental evidence to calculate the maximum probable rotation<sup>7</sup>;  $\varphi_T$  is a constant based on experimental evidence to calculate the maximum probable tension force in the vertical leg of the tension angle<sup>7</sup>.

## SIMPLIFIED SEISMIC ANALYSIS PROCEDURE FOR SLAB-ON-GIRDER CONCRETE BRIDGES

In order to develop a step by step analysis and design proposal for the ductile end-diaphragm system considers Fig. 4. In that figure, supports are shown as perfect steel hinge supports instead of the elastomeric bearings of the actual bridge. Besides, any contribution on the total displacement by the elastic deformation (flexure, shear element and shear panel) from the bridge beams is not considered

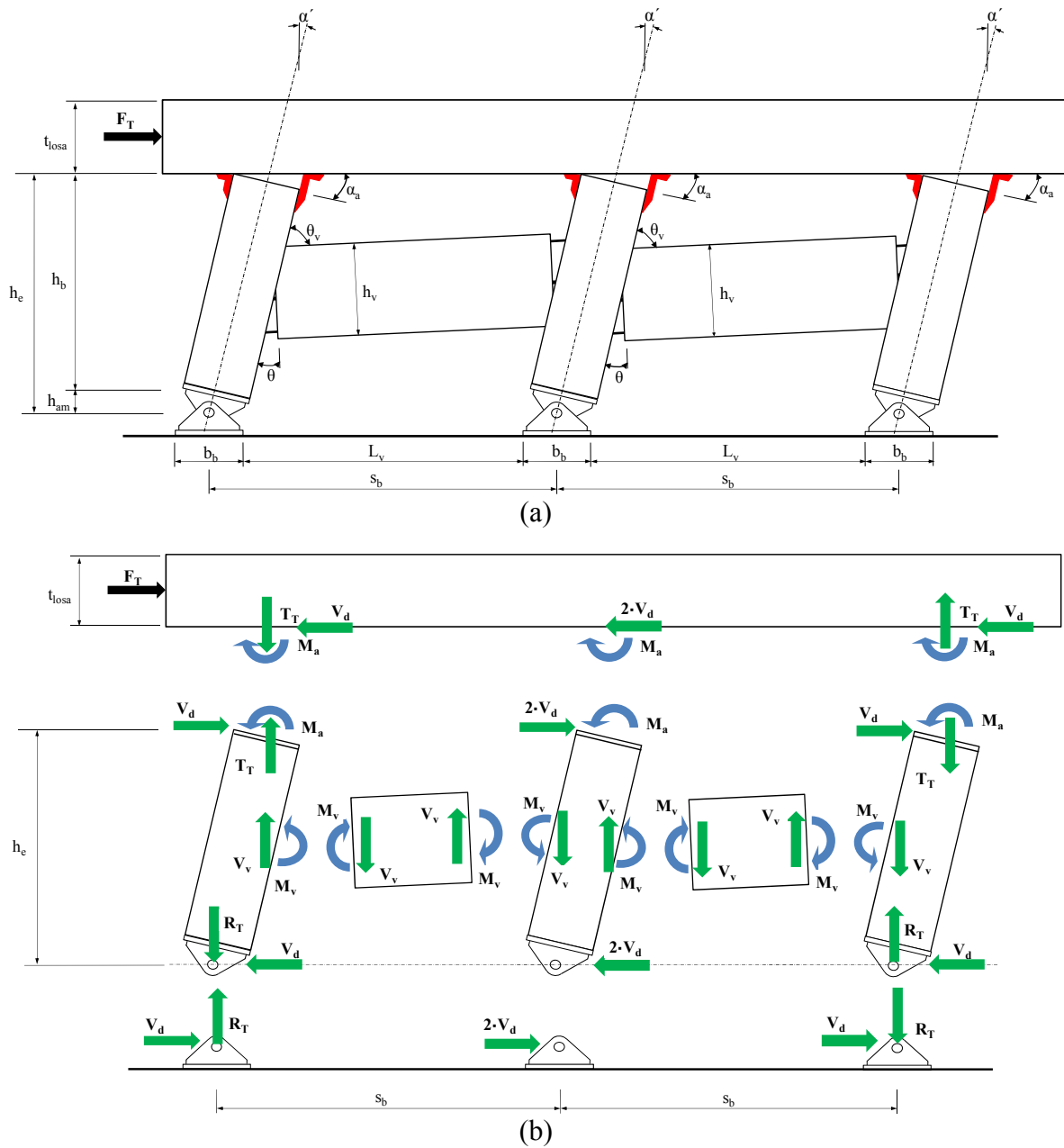


Fig. 4 Proposed simplified analysis of the ductile end-diaphragm system: (a) Kinematic; (b) Equilibrium.

Fig. 4(a) shows a schematic of the kinematic at one bridge's ends, and Fig. 4(b) shows the reactions that come from the application of seismic forces without taking into account any dead or live load. The term  $F_T$  refers to any force applied to the slab to represent, in a force based design, the seismic action whether elastic or inelastic.

Therefore, based on the proposal made by Zahrai and Bruneau<sup>1</sup> for steel bridges, the simplified seismic design procedure of slab-on-girder concrete bridges is describe by the following steps (All equations below in SI units):

*Step 1:* Consider the bridge as a simplified system of springs in series whose total equivalent stiffness is given by the following equation:

$$K_e = \frac{1}{\frac{1}{K^*} + \frac{1}{K_{extr}} + \frac{1}{K_{sub}}} \quad (11)$$

where  $K^*$  is the generalized lateral stiffness of the superstructure;  $K_{extr}$  is the total lateral stiffness of the end-diaphragm systems;  $K_{sub}$  is the lateral stiffness of the substructure including bearings, abutments, piers, foundations and soils. It should be verified that the value of  $K_{sub}$  is high enough to be ignored in Eq. 11 henceforth, in order to avoid unpractical ductility demands on the ductile diaphragm system<sup>1</sup>.

*Step 2:* In the case of a new design, choose the dimensions and constituent materials of the superstructure, and in the case of a retrofit project use the actual dimensions and constituent materials of the existing bridge.

*Step 3:* With the data from *Step 2*, calculate the generalized mass,  $m^*$ , and generalized lateral stiffness,  $K^*$ , both for the superstructure, assuming a single degree of freedom behavior and fundamental principles of dynamics of structures using a sine shape function with the following equations:

$$m^* = \frac{M}{2} \quad (12)$$

$$K^* = \frac{\pi^4 \cdot E_{cL} \cdot I_D}{2 \cdot L^3} \quad (13)$$

Where  $M$  is the total mass of the entire superstructure;  $E_{cL}$  is the modulus of elasticity of concrete's slab;  $I_D$  is the moment of inertia of the whole superstructure section about a vertical axis perpendicular to the deck.

*Step 4:* Obtain an initial estimate of the equivalent fundamental lateral period of the bridge omitting, only at this step, the contribution of  $K_{extr}$  in Eq. 11, and using the following equation where it is implicit the supposition that the weight of the substructure may be neglected:

$$T_e = 2 \cdot \pi \cdot \sqrt{\frac{m^*}{K_e}} \quad (14)$$

*Step 5:* Calculate the total lateral elastic shear,  $V_{\text{elast}}$ , by means of the following relationship, which can be derived by using fundamental principles of dynamics of structures and considering a sinusoidal shape function:

$$V_{\text{elast}} = S_a \cdot \left( \frac{8 \cdot M \cdot g}{\pi^2} \right) \quad (15)$$

Where  $S_a$  is the code specified seismic response coefficient for a return period of 1000 years.

The lateral shear for each end of the bridge,  $V_{\text{extr}}$ , is given by:

$$V_{\text{extr}} = \frac{V_{\text{elast}}}{(2)} \quad (16)$$

*Step 6:* Choose the reduction factor,  $R$ , and the respective value of ductility,  $\mu$ , taking into account the region of the response spectrum where the fundamental lateral period is located. A value of 2,25 is suggested for  $R$  in this project but it is required more research to determine a consensual value.

*Step 7:* Determine the value of the inelastic seismic shear for each end,  $V_{\text{inel}}$ , by means of the following equation:

$$V_{\text{inel}} = \frac{V_{\text{extr}}}{R} \quad (17)$$

*Step 8:* By equilibrium of Fig. 4(b), calculate the transverse force,  $V_d$ , setting the force  $F_T$  equal to the value  $V_{\text{inel}}$  calculated by Eq. 17.

*Step 9:* Considering that at the middle of the diaphragm by symmetry the moment is zero, it is possible to derive Eq. 18. Assuming that the moment resistance at the rocking beam-to-slab joint,  $M_a$ , is zero (which is reasonable given its little relative value compared to the others parameters), calculate the value of shear resistance at the hybrid diaphragm-to-beam joint,  $V_v$ , utilizing Eq. 18:

$$V_d = \frac{\left( \frac{V_v \cdot s_b}{2} + M_a \right)}{h_e} \quad (18)$$

where  $h_e$  is the effective height of the bridge's cross section.

With the value of  $V_v$ , design the hybrid diaphragm-to-beam joint and obtain the force-displacement relationship by means of Eqs. 1 to 5.

*Step 10:* Calculate  $M_a$  for the rocking beam-to-slab joint so that the entire ductile end-diaphragm system has re-centering capability. In order to achieve this, the following requirement should be met:

$$M_a \leq M_{\text{prs}} - M_{\text{su}} \quad (19)$$

where  $M_{pr_s}$  is the maximum probable moment capacity of the unbonded post-tensioning steel of the hybrid joint;  $M_{su}$  is the maximum probable moment capacity of the mild steel reinforcing steel of the hybrid joint.

With the value of  $M_a$ , design the rocking beam-to-slab joint and obtain the moment-rotation relationship by means of Eqs. 6 to 10.

*Step 11:* Calculate the total lateral stiffness of the end-diaphragm systems,  $K_{extr}$ , as the sum of all the ductile end-diaphragm system's stiffness,  $K_{SDD}$ , determined by the following relationship:

$$K_{SDD} = \frac{(2 \cdot n - 2) \cdot \left[ \frac{K_{iv} \cdot L_v \cdot s_b}{2} + \frac{K_{ia\alpha}}{(1 + \Omega) \cdot \left(1 + \frac{b_b}{L_v}\right)} \right] \cdot \left(1 + \frac{b_b}{L_v}\right)}{h_e^2} \quad (20)$$

where  $n$  is the number of bridge beams;  $s_b$  is the beam bridge spacing;  $\Omega$  is used to take into account the influence of the flexibility of the precast concrete slab in the overall stiffness. The term  $K_{iv}$  is calculated using Eq. 3, and  $K_{ia\alpha}$  is calculated using Eq. 8.

*Step 12:* With  $K^*$  and  $K_{extr}$  values, calculate  $K_e$  using Eq. 11. With  $K_e$  and  $m^*$  values, calculate  $T_e$  using Eq. 14. Calculate  $V_{elast}$  again using Eq. 15, and finally  $V_{extr}$  using Eq. 16.

*Step 13:* Calculate the design elastic displacement.

*Step 14:* By the "equal displacement" approximation obtain the design value of  $V_{inel}$  and calculate the value of  $R$  using Eq. 17. Compare with the initial proposed value in *Step 6* and if necessary modify the ductile end-diaphragm system as required and go back to *Step 11*.

*Step 15:* As a maximum, the value of  $V_{inel}$  should be half the lateral resistance of substructure.

*Step 16:* The maximum probable lateral drift of the bridge, calculated utilizing the yield displacement and the value of  $\mu$  associated to  $R$ , should be less or equal to 1%.

## CASE STUDY

In order to test the proposed solution of precast ductile diaphragms, a hypothetic structure that meets the dimensional and materials characteristics of typical bridges in Costa Rica, Central America, is proposed. There is a standard schematic of concrete precast/post-tensioned bridge with lengths ranging from 22m to 28m, that was and is still widely used since the late 60's. The dimensions of this standard bridge will be used for the case study.

The bridge has a length between supports of 28m and a total length of 28,4m, and it is composed of three concrete precast/post-tensioned beams; the beam spacing is 2,44m; the precast beams are 1,52m in height and 0,48m in width; the haunch thickness is 0,03m; the concrete deck is precast with a thickness of 0,19m (including a 0,01m riding surface) and 6,12m wide. The concrete precast diaphragms are 0,65m in height, 0,25m in width, and 1,93m length. In the joint between diaphragms and bridge beams there is a tolerance spacing of 0,015m.

The concrete precast deck has a compressive strength of 42MPa. Both the haunch, and the gap between bridge beams and diaphragms, as well as the block-outs in the precast deck panels, are filled with high performance non-shrinkage grout with a compressive strength of 70MPa. The concrete compressive strength of the bridge beams is 70MPa, and in the case of the diaphragms is 42MPa. This is because in order to protect the bridge beam concrete from crushing and spalling failure, it has to have a compressive strength greater than the maximum confined concrete resistance of the diaphragms. The mild steel reinforcement is ASTM A706 and the post-tension strands are ASTM A416 low relaxation steel.

Fig. 5 shows the sequential construction stages of the proposed solution. It could be the case of the retrofit of an existing bridge, so it is necessary to change the entire superstructure or only substitute the CIP slab by a precast concrete deck, in both cases to protect the substructure from seismic damage. It could be too the case of a new 100% precast concrete bridge.

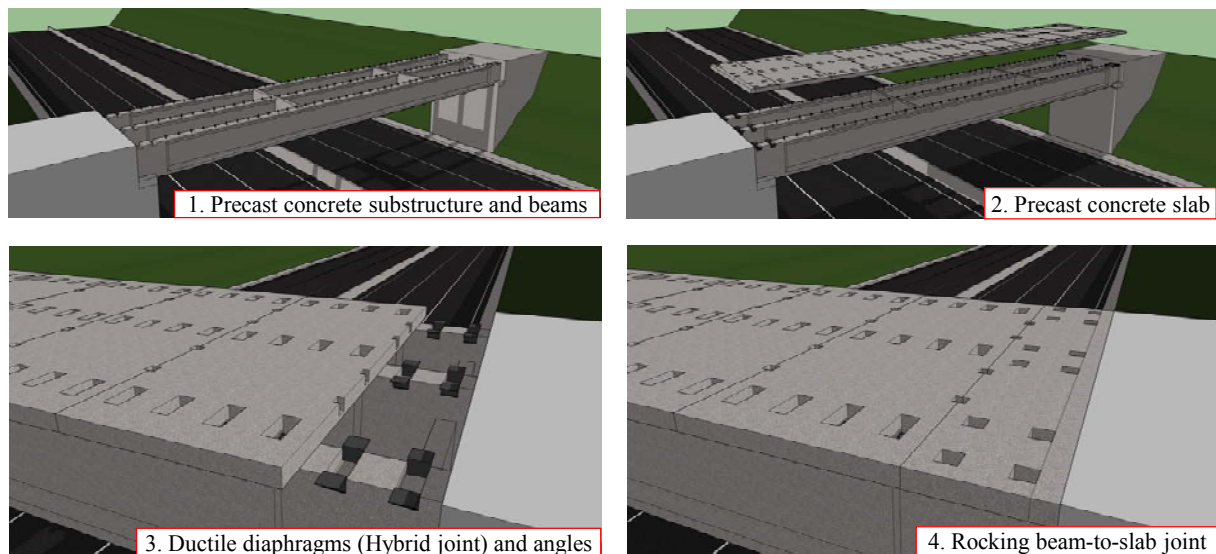


Fig. 5 Sequential constructive stages of the case study bridge.

Once the bridge beams are placed, the placing of the precast concrete panels begins. At the same time the ductile diaphragms are located at the ends and the steel angles are located at its

final position. It is proposed to leave block-outs at the top of the precast beams in order to increase the constructive tolerances, however the possibility of pre-installing the connections bolts in the precast beams can be evaluated. These bridge beam's block-outs are fill with self-compacting concrete. The ends panels are placed again, the precast deck is longitudinally post-tensioned, and finally the haunch and panel's block-outs are filled with the high performance grout. Notice that Fig. 5 schematically shows two set of angle connections per beam, but the actual necessary amount need further research.

Fig. 6 shows the case of the simplified seismic design procedure applied to one of the bridge case study's ends. The figure shows most of the main parameters that characterize the ductile diaphragm system behavior. As noted, in this case the steel angles are kept in the elastic range even for the maximum drift limit level, situation that could be changed during the design process in order to modify the dissipation energy characteristic of the system.

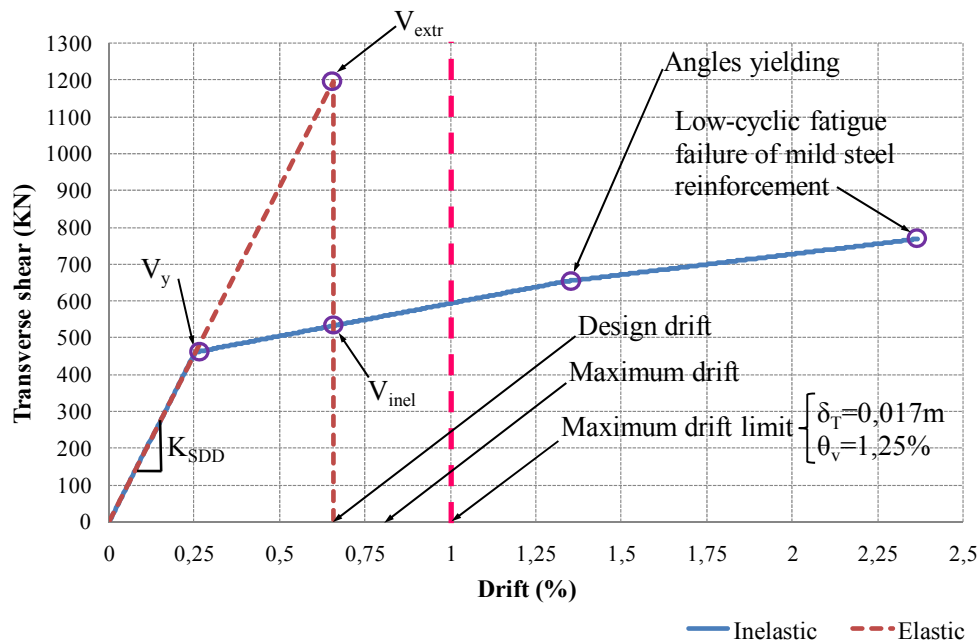


Fig. 6 Simplified seismic design procedure applied to case study.

### LABORATORY TEST SETUP

In order to test the ductile diaphragm system applied to the case study using the simplified seismic design procedure, a 0,60m end section of the bridge as it is shown in Fig. 7 is selected and it full scale testing will be performed at LanammeUCR facilities.

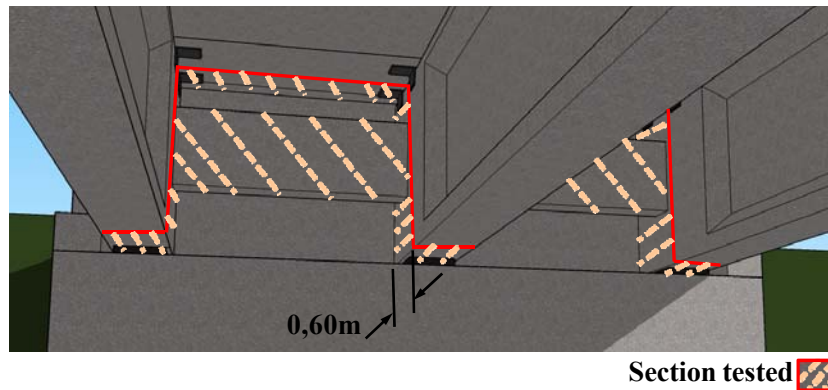


Fig.7 Section of the bridge case study to be tested at LanammeUCR of the University of Costa Rica.

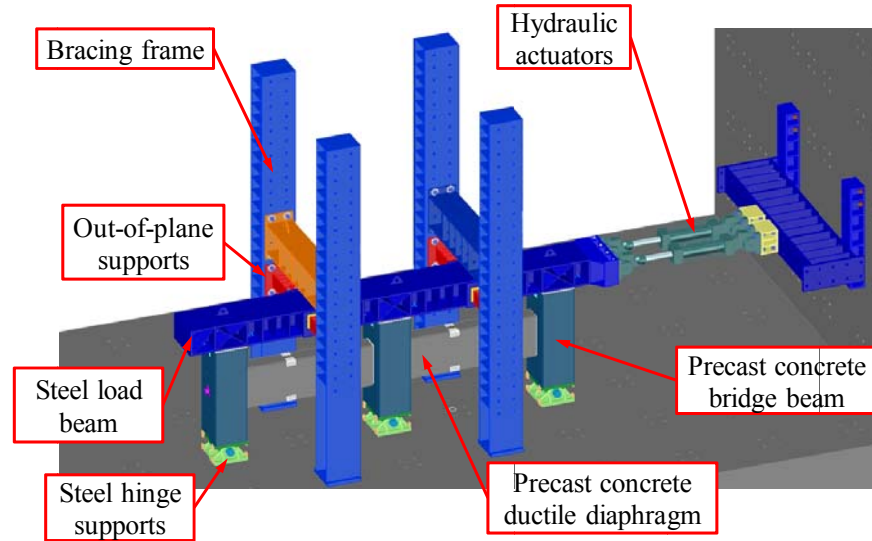
Fig. 8(a) shows the test set up proposal for the experiment and Fig. 8(b) shows the progress of construction in the laboratory to date.

The bracing frames shown in Fig. 8(a) act together with the out-of-plane supports to avoid any displacement of the specimen different from the line of action of the actuators. In the out-of-plane supports PTFE sliding surfaces will be used.

The specimen will be subjected to progressively increasing cyclic lateral displacement following ACI ITG-5.1-07<sup>8</sup> protocol as closely as possible. There will be no applied dead load except for the self-weight of elements. Two MTS actuators will be used to apply the lateral force. The specimen will be instrumented for displacement and strain measurements at the points of interest with a total of 33 electrical resistance strain gauges and 20 linear displacement transducers. A load cell in the post-tensioning steel anchor will be used to measure the actual anchor set loss at prestress transfer and to verify that strands will not yield during the test.

As noted in Fig. 8, instead of using elastomeric bearings in the supports as in the actual case study, steel hinge supports whose purpose is to act as perfect simple supports and at the same time to keep the equilibrium of the test by resisting the lift force at external beams due to the lateral seismic force plus the absence of superstructure dead load are used.

In similar tests carried out on end diaphragms (ductile or not) for steel bridges, actual concrete slab were used and the seismic force was applied to it by hydraulic actuators. The last implies that when test is performed, the concrete slab is subjected to high tension-compression longitudinal forces, which could induce cracking on the slab much before it will take in a real earthquake, with consequences like damage and decrease in stiffness among others that do not represent the actual behavior. In order to avoid this scenario, a strong steel load beam with a considerable higher stiffness than the precast concrete deck is used.



(a)



(b)

Fig.8 Test set up for the test at LanammeUCR: (a) Final test set up proposal; (b) Progress of construction to date.

Fig. 9 compares the theoretical Force-Drift curves derived for case study and test proposal using the simplified analysis procedure in both cases. As shown, the main consequence of using the strong steel load beam is that the angles yield before they would do it with a more flexible slab as in case study bridge. This could be seen from two points of view: in the test the steel angles become more effective in the energy dissipation contribution, and in the case study the steel angles are protected against inelastic behavior for most of the resistance drift and therefore protected against damage.

Once the test has been executed, a Force-Drift hysteresis experimental curve will be obtained, and the backbone curve will be derived for both positive and negative drift. Finally, that envelope curve will be compared with the theoretical test curve from Fig. 9 in order to verify the suitability of the simplified analysis procedure in predicting the end's transverse section behavior.

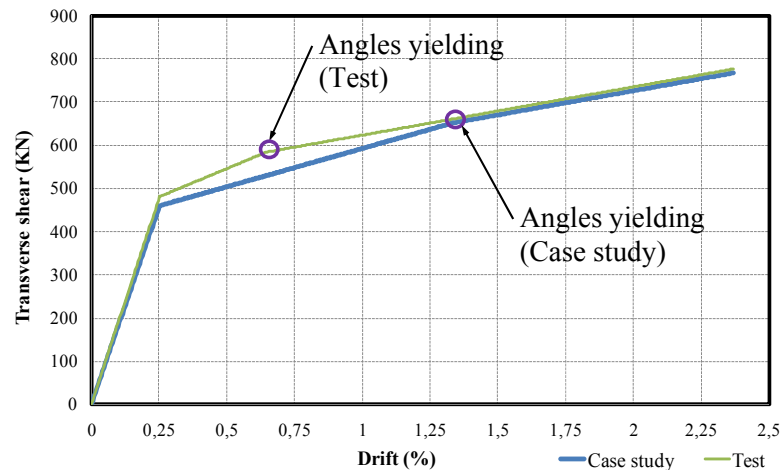


Fig. 9 Comparison between the theoretical results from the case study and experimental test proposal.

## CONCLUSIONS

1. In order to retrofit existing concrete bridges, by changing the entire superstructure or only substitute the CIP slab by a precast concrete deck, or design new structures in moderate-to-high seismic risk zones, it is possible to come up with the alternative possibility to use ductile end diaphragms as part of ABC solutions.
2. It is possible to predict the behavior of the ductile end diaphragm system by taking into account the kinematic, materials constitutive laws and the equilibrium of joints and in general of the overall behavior of bridge end's cross section, and then to simplify the analysis using a step-by-step procedure to seismically design the bridge.
3. Taking the geometry and materials characteristics of a very common precast/prestressed bridge used in Costa Rica, it is possible to apply the ductile end diaphragm system to a hypothetical case study and solve most of the constructive and practical issues.
4. The test of the end diaphragm system will allow obtaining experimentally the actual force-drift behavior and compare it with the theoretical behavior of Fig. 9. The correlation between both curves will allow the researchers to conclude on the effectiveness of the simplified seismic analysis procedure.

5. The test performance of the end diaphragm system as well as the measurements, will verify the practical effectiveness of the proposed solution for seismic resistance.

## REFERENCES

1. Zahrai, Seyed M. and Bruneau, Michel, "Ductile End-Diaphragms for Seismic Retrofit of Slab-on-Girder Steel Bridges", *ASCE Journal of Structural Engineering*, Vol. 125 (1), January 1999, p.p. 71-80.
2. Zahrai, Seyed M. and Bruneau, Michel, "Cyclic Testing of Ductile End Diaphragms for Slab-on-Girder Steel Bridges", *ASCE Journal of Structural Engineering*, Vol. 125 (9), September 1999, p.p. 987-996.
3. AASHTO, "AASHTO Guide Specifications for LRFD Seismic Bridge Design", *American Association of State Highway and Transportation Officials*, 2° Ed. Washington, DC:, 2011.
4. Yen, Wen-Huei Phillip et al., "Post-Earthquake Reconnaissance Report on Transportation Infrastructure: Impact of the February 27, 2010, Offshore Maule Earthquake in Chile", *FHWA*, Publication No. FHWA-HRT-11-030, October 2011, pp. 29- 90.
5. Celik, O. and Sritharan, S. "An Evaluation of Seismic Design Guidelines Proposed for Precast Concrete Hybrid Frame Systems", *Precast/Prestressed Concrete-Manufacturers Association of California-University of Iowa*, ISU-ERI-Ames Report ERI-04425, January 2004.
6. Restrepo, José I. and Rahman, Amar, "Seismic Performance of Self-Centering Structural Walls Incorporating Energy Dissipators", *ASCE Journal of Structural Engineering*, Vol. 133 (11), November 2007, p.p. 1560-1568.
7. Weldon, Brad D. and Kurama, Yahya C.; "Experimental Evaluation of Posttensioned Precast Concrete Coupling Beams", *ASCE Journal of Structural Engineering*, Vol. 136 (9), September 2010, p.p. 1066-1077.
8. ACI Innovation Task Group 5, "ACI ITG-5.1-07: Acceptance Criteria for Special Unbonded Post-Tensioned Precast Structural Walls Based on Validation Testing and Commentary", *ACI American Concrete Institute*, March 2008.